

# Calculation of gamma ray attenuation coefficients for some locally manufactured PVA shielding materials

**Khawla Ahmed Muheisen**

*Department of Physics, College of Science, University of Wasit, Iraq,  
khwlh849@gmail.com*

**Hadi D. Al-Attabi**

*Department of Physics, College of Science, University of Wasit, Iraq.*

## Abstract

In this study, the mass attenuation coefficient (mm) of a locally developed shielding material was calculated analytically, polyvinyl alcohol. When compared to the photon energy range values received from the, a Windows version of the XCOM database 0.001MeV 10000MeV. These two values have a high degree of agreement . The calculated(mm) values have been displayed together with their fluctuations with photon energy. In contrast, the following four shielding materials. The obtained results show that  $\mu_m$  are highly dependent on Photon energy is a type of energy. The chemical make-up and density of the shielding materials.

**Keywords:** *Gamma rays, Attenuation, Shielding, Radiation Polymeric materials.*

## 1. INTRODUCTION

As nuclear technology progresses, so do the numerous positive applications of various radiation types used in medicine, industry, agriculture, and research, as well as nuclear power production. Yet, one downside of these peaceful applications of radiation is that it makes employees who work in institutions that use this type of radiation source, including other humans, at risk of exposure. When any tissue of any organ in the body is exposed to a high amount of radiation, the chemical nature of the cell changes as a result of the ionization of its atoms, and thus this cell may be exposed to death As a result, it is critical to limit the amount of radiation to which the body's cells are subjected by shielding the body with a biological shield made of materials with a high ability to stop or weaken the radiation to which the body is exposed. To manufacture any biological shield, it is very important to know its nuclear, structural, and physical

qualities, as well as the properties of the radiation to which this sort of shield is subjected. The nuclear coefficients that must be known in order to design and select the material of any radiation-protective shield are the total mass attenuation coefficient (m) and the linear attenuation coefficient (l), and we will discuss how to calculate them later. [1] To reduce the harm of radiation, people who are close to radiation sources, whether in hospitals or otherwise, use protective shields made of high-density lead material, which makes this type of shield very heavy, as the weight of the shield reaches from 30 to 35 kg, so it is difficult for the human body to wear a shield of this weight As a result, we created shields from natural materials that are light in weight, cheap in cost, of equal quality, and have superior mechanical and radiological properties. These materials are natural polymers like maize starch and chitin that we grafted with cement and tungsten powder in

specific proportions. Where we studied the nuclear properties of these polymeric materials, specifically, we calculated the attenuation coefficients and the stopping power practically and theoretically to make sure that they match the required specifications, as the results showed that the theoretical calculations matched the practical results to a very acceptable degree. Several scientific, engineering, and medical applications require information on the scattering and absorption of photons (X-rays, gamma rays, and sunlight). The number of materials that require photon absorption cross-sections is enormous and continues to rise. From a scientific standpoint, printed tables cannot adequately meet all optical absorption cross-section requirements. Furthermore, cross-sections at photon energies other than those listed in the tables are frequently required. The photon cross-sections of the compounds can, of course, be calculated exactly as a weighted sum of the atomic component cross-sections (save for energies around absorption edges). The numerical work required, however, is time-consuming and intricate. The procedure is further complicated by the fact that the optical absorption cross-sections and overall attenuation coefficients do not remain constant at the absorption edges. Because of the presence of these discontinuities, it is preferred to include photon energies just above and below all absorption edges for all atomic components in the composite cross-section tables. Therefore, a suitable alternative must be found so that we can generate as needed, cross-sections and attenuation coefficients for compounds and mixtures. This job can be done using XCOM software for any element, compound, or mixture with energies ranging from 1 keV to 100 GeV. Cross-sections can be generated by XCOM at particular energies, user-specified energies, or both. At energies directly above and below all absorption edges, cross-sections are automatically added. XCOM generates

two types of output: (a) tables that are most closely related to tables identified in published studies; (B) Graphical representation of tabulated statistics. Whole cross-sections, attenuation coefficients, and partial cross-sections are given for the following processes: inhomogeneous dispersion, homogeneous dispersion, photoelectric absorption, and pair formation in the fields of atomic nuclei and atomic electrons. The compounds' tabulated numbers are partial total reaction coefficients, which are the product of the respective cross-sections multiplied by the number of target particles per unit mass of the substance. The mean free pathways between scattering, photoelectron absorption, and pair formation events are the reciprocal equations for these interaction coefficients. The total attenuation coefficient is equal to the sum of the interaction coefficients of the separate processes. Because it is frequently employed in gamma ray transmission calculations, The overall attenuation coefficients are also given without the contribution from homogenous dispersion. The total of the atomic component quantities is used to compute the reaction coefficients and the sum of the attenuation coefficients for compounds or mixtures. Based on the chemical formula provided by the user, XCOM determines weighting factors, or fractions by weight of constituents. Blends, on the other hand, require the user to define weight percentages of the individual constituents.[2]

## 2. Attenuation of Gamma Radiations

The mass attenuation coefficient (obtained by dividing the linear attenuation coefficient by the absorbed density) is actually more important than the linear attenuation coefficient. This is due to the fact that all mass attenuation coefficients are independent of the absorbent's density and physical condition (gaseous, liquid, or solid). Furthermore, when  $Z/A$  is  $0.45 \mp 0.05$ , the mass attenuation coefficient is almost independent of the atomic

number, where  $Z$  = effective atomic number and  $A$  = effective mass number of the absorber.[3] Moreover, the mass attenuation coefficient facilitates easy comparison of the radiation shielding efficiencies of the shielding materials.

Calculating the total mass attenuation coefficient:

When a gamma ray beam passes through an absorbing material, the radiation intensity will be attenuated according to BeereLambert's Law .[4]

$$I = I_0 e^{-\mu_m} = I_0 e^{-(\mu \backslash \rho) t_d} = I_0 e^{-\mu_m t_d} \dots \dots \dots (1)$$

$\mu$  is the intensity of the unattenuated and attenuated gamma rays, is the linear attenuation coefficient,  $I, I_0$ . The mass attenuation coefficient  $\mu \backslash \text{cm}^2, t_d$ , is the thickness in cm And the relationship between  $\mu$  and  $\mu_m$  is given by the following equation:

$$\mu = \mu_m \times \rho \dots \dots \dots (2)$$

The total mass attenuation coefficient,  $(\mu \backslash \rho)_{\text{Compound or mixture}}$  of any chemical compound

A mixture of elements that can be calculated by dividing the linear attenuation coefficient by the absorbed density. [4]

$$\mu \backslash \rho_{\text{Compound}} = \sum_i (\mu \backslash \rho)_i W_i \dots \dots \dots (3)$$

where  $W_i$  and  $(\mu \backslash \rho)_i$  are the weight and mass attenuation coefficient of the element, respectively. For a chemical compound, the value of  $W_i$  can be calculated by the following equation:

$$W_i = \frac{n_i A_i}{\sum_j n_j A_j} \dots \dots \dots (4)$$

Where  $A_i$  is the atomic weight of the element and  $n_i$  is the number of formula units and

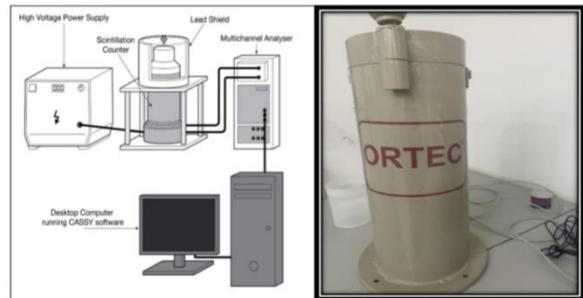
$$\sum_i W_i = 1 .$$

### 3. MEASUREMENT SYSTEM

It is possible to determine the concentrations of natural radioactive elements in the samples after detecting the gamma rays resulting from these elements or their radioactive offspring,

using an appropriate technique that suits the case studied, as many efficient techniques are available to achieve this work. One of the most important of these techniques is the gamma ray spectroscopy technique (gamma spectroscopy), which is based on a basic rule represented in the interaction of the beam with the detector material. This technique is distinguished by its great efficiency and energy separation. The most commonly used detection system is the thallium-doped sodium iodide detector system (NaI (TI) It is a solid and transparent organic scintillation detector that is characterized by its low cost, sensitivity, and high efficiency, as well as the fact that it works at room temperature, but its analysis capacity is limited. Because of its sensitivity and great efficiency, this method is regarded as one of the best for measuring and analyzing natural radioactive elements. In this study, a sodium iodide detector system was used at Al-Ain Private University in Thi-Qar Governorate to detect, measure and analyze radioactive properties in samples of polymeric materials of natural origin.

**Figure (1) Scheme of the gamma spectroscopy system used in the current study.**



One of the first gamma detectors used in spectroscopy was NaI(Tl) scintillation. Even now, several decades after its inception, it remains the best choice for an external gamma spectrometer due to its combination of cost-effectiveness and reliability. [5]

Nuclear radiation detectors have become one of the most basic devices as radiation detectors due to the use of radioactive sources in a variety of fields such as health physics, industrial, energy, and environmental applications. Individual wellbeing is endangered. In radiometric, a solid grasp of detector spectrum performance is critical. Detectors are not completely efficient because radiation can travel considerable distances between detector contacts before detection is feasible. One of the most significant characteristics of a detector is its ability to measure radiation. The gamma spectrometer is a common detection instrument in this field, and its performance is closely related to understanding detection efficiency. The recognition effectiveness The percentage of radiation detected by a particular detector in relation to the total yield produced by the source. They differ depending on the detector material's size and shape, its absorption cross-section, the attenuation layers in front of the detector, and the distance and position between the source and the detector. [6]. Small amounts of impurities called triggers are introduced into the crystal to enhance the photon emission potential and reduce the self-absorption of light. Because thallium is a frequently used activator, these reagents are classified as NaI (Tl). The activator fills the energy gap with states, Between activated states, light is emitted. The maximum emission wavelength of NaI was modified from 303 to 410 nm in pure NaI. Absorption cannot occur at this energy because the doping ground states in NaI(Tl) are empty. The change in wavelength from ultraviolet to visible causes more overlap with the maximum sensitivity of most photomultiplier tubes. [7]. The structure of the NaI(Tl)

detector is depicted in Figure (1). It is made up of a single crystal of thallium-doped sodium iodide that is optically linked to a photomultiplier tube's photocathode. When gamma rays hit the detector, sodium iodide ionizes. This causes excited states in the crystal to decay by releasing photons of visible light. This form of emission is referred to as luminescence.[8]

The incoming radiation penetrates the detector and is subjected to a plethora of interactions, which excite the atoms.

- Because excited states rapidly create visible or near-visible light, matter is said to fluoresce.
- When light strikes a photosensitive surface, only one photoelectron per photon is emitted..
- These secondary electrons are amplified, accelerated, and modulated into the output pulse by the photomultiplier tube (PM).
- Depending on the application, scintillators and PM tubes appear in a variety of shapes and sizes. [9].

#### 4. Results and discussion

Introduction:-

In our current study we calculated the theoretical and practical values of the mass attenuation coefficient,  $\mu \rho$  ( $[\text{cm}^2/\text{g}]$ ) It was represented by 14 samples of various concentrations of polyvinyl alcohol (PVA) polymer, which was created locally, where we theoretically calculated the concentrations of different substances for heterogeneous samples using equations for different chemical elements. (1-4) at a photon energy ranging from 0.001 MeV to 100000 MeV.

**Table (1):- shows the sample code, its chemical formula, and concentration of the materials used.**

Concentration sample	Chemical formula	Sample	No.
0.85+0.10+0.05	C2H4O+ C56H103N9O39+ ,Ca2SiO4	C1	1
0.80+0.10+0.10	C2H4O+ C56H103N9O39+ ,Ca2SiO4	C2	2
0.75+0.10+0.15	C2H4O+ C56H103N9O39+ ,Ca2SiO4	C3	3
0.90+0.10	C2H4O+C56H103N9O39	Control	4
0.75+0.225+0.025	C2H4O+C56H103N9O39+W	E1	5
0.75+0.20+0.005	C2H4O+C56H103N9O39+W	E2	6
0.75+0.175+0.075	C2H4O+C56H103N9O39+W	E3	7
0.75+0.20+0.05	C2H4O+C6H10O5+Ca2SiO4	M1	8
0.70+0.20+0.10	C2H4O+C6H10O5+Ca2SiO4	M2	9
0.65+0.20+0.15	C2H4O+C6H10O5+Ca2SiO4	M3	10
0.75+0.225+0.025	C2H4O+C6H10O5+W	T1	11
0.75+0.20+0.05	C2H4O+C6H10O5+W	T2	12
0.75+0.175+0.075	C2H4O+C6H10O5+W	T3	13
0.90+0.10	C2H4O+C6H10O5	Control	14

The X-com program was then used to determine the total mass attenuation coefficient of the aforementioned samples for the energy range 0.001-100000 MeV, allowing us to compare experimental and theoretical findings. For a sampling of materials, the values of  $\mu_m$  were also computed for the photon energy of certain typical gamma ray sources.

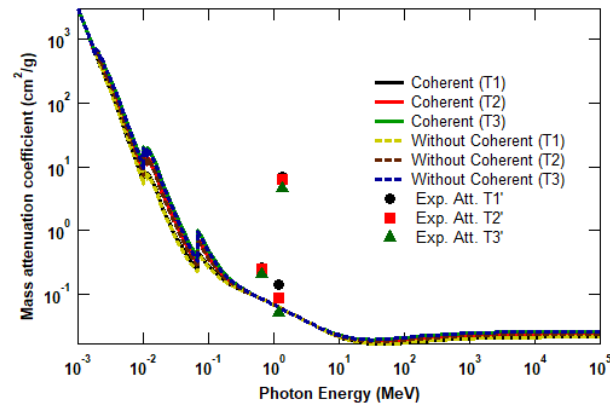
Total mass attenuation coefficient  $\mu_m$

Figure (1-7) shows the experimentally calculated values of the total mass attenuation coefficient,  $\mu_m$  ( $[\text{cm}]^2/\text{g}$ ) and the X-com values for the fourteen shielding samples for the gamma-ray energy range, which ranges from 0.001MeV to 100000MeV.

Figures (1-7) show that the total mass attenuation of gamma rays depends on the energy of the incident photon and the chemical

composition of the absorbent material, as the value of the mass attenuation decreases with the increase in the energy of the incident photon.

**Figure (4.1):** Mass attenuation coefficient of the sample (T) for heterogeneous materials of different concentrations as a function of photon energy.



**Figure (4.2):-** sample mass attenuation coefficient (M) for heterogeneous materials of different concentrations as a function of photon energy.

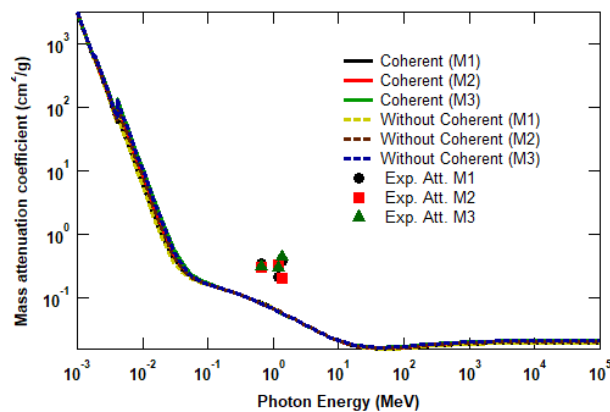


**Figure (4.3):** Mass attenuation coefficient of the sample (C) for heterogeneous materials of different concentrations as a function of photon energy.

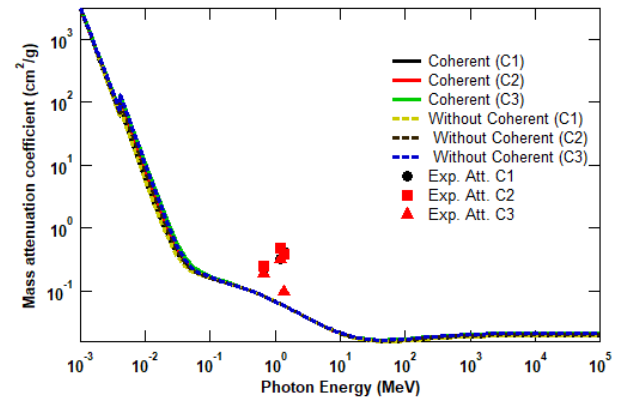


**Figure (4.4):** Mass attenuation coefficient of the sample (E) for heterogeneous materials of different concentrations as a function of photon energy.

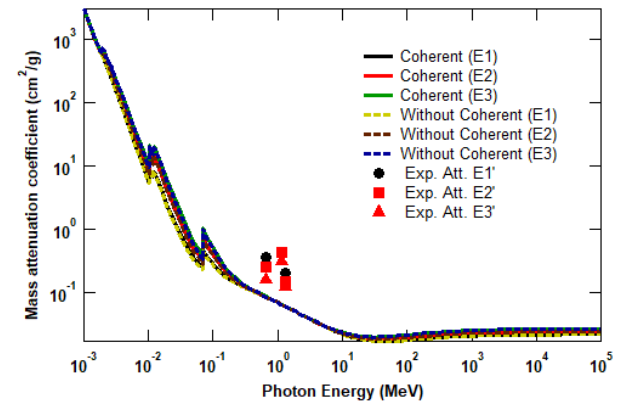


**Figure (4.5):** Mass attenuation coefficient of the sample (Control 1 and Control 2) for heterogeneous materials of different concentrations as a function of photon energy.

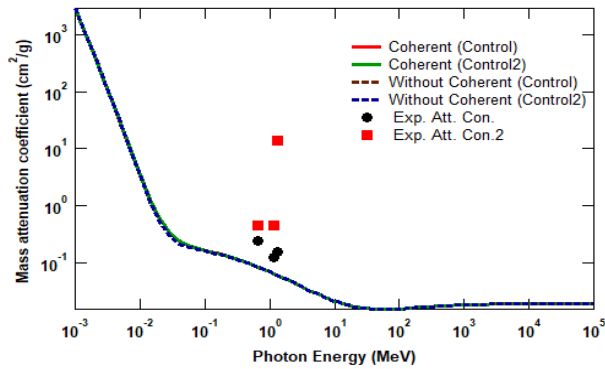


**Figure (4.6):-** Mass attenuation coefficient for Control 1, Control 2, C, E, M, T samples (without coherent scattering) for inhomogeneous materials of different concentrations as a function of photon energy.

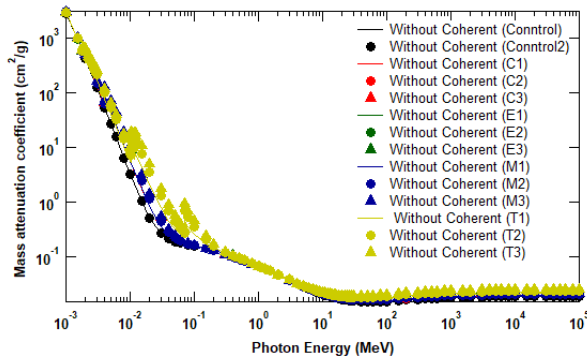
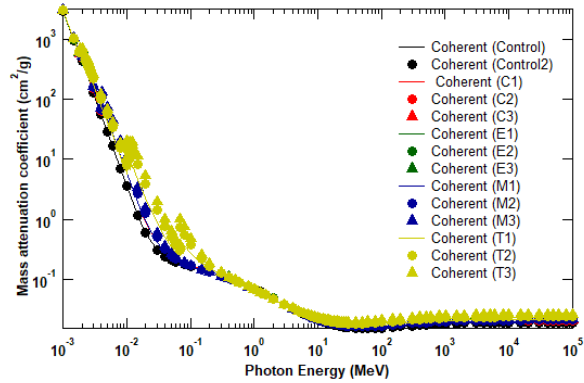


**Figure (4.7):-** Mass attenuation coefficient for Control 1, Control 2, C, E, M, T samples in the presence of coherent dispersion of inhomogeneous materials of different concentrations as a function of photon energy.



Figures (1-7) show us that the total mass attenuation coefficient as a function of the photon energy for the sample T is higher than the rest of the other samples at the energy range from 0.001MeV to 0.0025MeV. With the exception of the very low energy range through these figures, The mass attenuation coefficient of the sample T achieves a maximum at around 0.0015MeV photon energy and then decreases as photon energy increases. (i.e. the peak attenuation coefficient is observed at about 0.0015 MeV). The T sample has the largest mass attenuation coefficient because it contains elements with a high atomic number, which are extremely effective at attenuating gamma rays. This is due to the effect of gamma rays on the photoelectric phenomena of materials, the interaction of generating pairs, and the Compton effect, which dissipates the energy of the incident photon. At low photon energy and high absorption atomic number, the photoelectric effect outperforms the other two interactions. The T sample has the highest mass attenuation coefficient in the low energy range due to the photoelectric effect. When the energy of the incoming photon is equal to the ionization or binding energy of the absorbed electron in the atom, Then the probability of

removing the electron (ie the photoelectric cross section) is the highest. The maximum value of the total mass attenuation coefficient is an indicator of the minimum photon energy required to decouple electrons.

Where the maximum value of the mass attenuation coefficient of the sample T is the result of the absorption edge of the K shell of the elements, C<sub>2</sub>H<sub>4</sub>O, W, C<sub>6</sub>H<sub>10</sub>O<sub>5</sub> with high atomic number. From Figure (1-7) it is clear to us that the mass attenuation coefficient of the sample M is slightly less than that of the sample T but greater than that of the sample C at the photon energy range from 0.001 MeV to 0.125 MeV. As a result, the concentration of the M sample and the atomic number of its elements are less than the concentration of the T sample and the atomic number of its elements is less, but the M sample has a higher concentration than the C sample and the atomic number of its elements is greater. So in this range of energy, the shielding properties of sample T for gamma rays are much better than those of sample M. The samples are arranged according to the decreasing mass attenuation coefficient according to each material within the aforementioned energy range as follows,

T>M >C >E > Control

From figure (1-7) we notice that as the photon energy increases .As the photon energy exceeds 0.125 MeV, the total mass attenuation coefficient drops (due to the photoelectric phenomena). The mass attenuation coefficient for all materials approaches a constant value for a specific energy range, and this is because the Compton scattering phenomena predominate in this energy range. In addition, for all elements on which the attenuation coefficient is dependent, the atomic number-to-atomic-weight ratio ( $Z/M$ ) is calculated. With the exception of hydrogen and heavier elements, the mass is nearly half. (John et al., 1967). This indicates that at this energy level, when Compton scattering is dominant, the

values of the attenuation coefficient are practically identical for all elements and materials with similar gamma-ray attenuation qualities. Pair production begins to dominate all samples as the photon energy exceeds 1.02 MeV, and its dominance grows as the photon energy increases, and it is also responsible for the entire increase in the mass attenuation coefficient. For the reasons stated above , in Figure (1-7) It is obvious that all of the sample materials have roughly the same mass attenuation coefficient over the photon energy range from 0.125 MeV to 6 MeV.

To illustrate the aforementioned phenomena, figures (8-21) were drawn, whose values were adopted from a program The X-COM, where it represents the variation of the mass attenuation coefficient of the studied samples with the difference of the photon energy for the total and partial input processes. It turns Photoelectric absorption predominate in both coherent and incoherent scattering events (Compton effect) at very low photon energy ranges for a particular energy range, beyond which the Compton effect becomes the dominant interaction until the energy end (20 MeV) From Figure (8-21) we also notice that the pair production starts at 1.02 MeV energy.

**Figure (4.8): Mass attenuation coefficient,  $\mu_m$  ( $[cm]^2/g$ ) as a function of the incident photon energy for sample( T1: PVA 0.75 + Starch 0.225 + Tungsten 0.025)) for the total and partial interactions.**

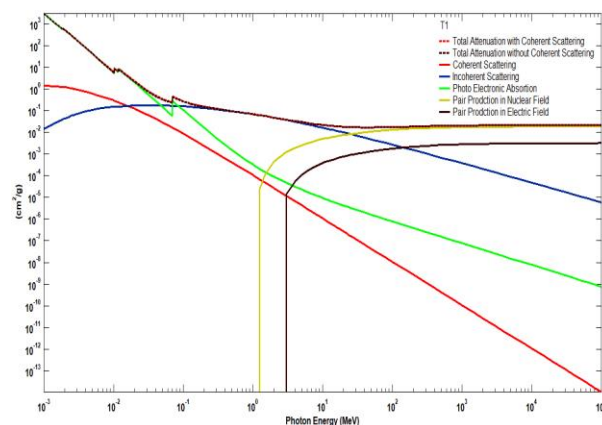


**Figure (4.9):** Mass attenuation coefficient,  $\mu_m(cm^2/g)$  as a function of the incident photon energy for sample( T2: PVA 0.75 +St 0.20 +W 0.05) for the total and partial interactions.

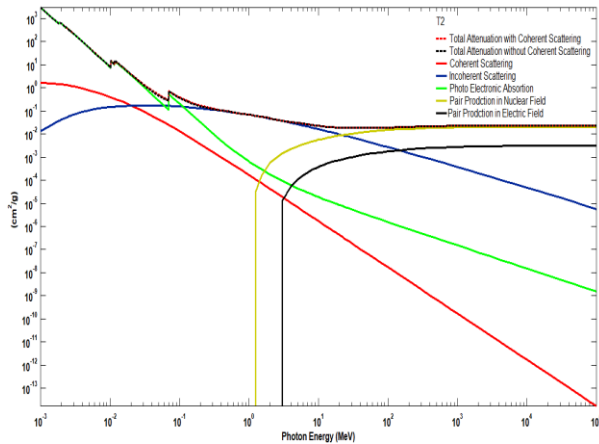


**Figure (4-10):** Mass attenuation coefficient  $\mu_m(cm^2/g)$  as a function of the incident photon energy for sample T3: PVA0.75 + St 0.175 + W 0.075)) for the total and partial interactions.

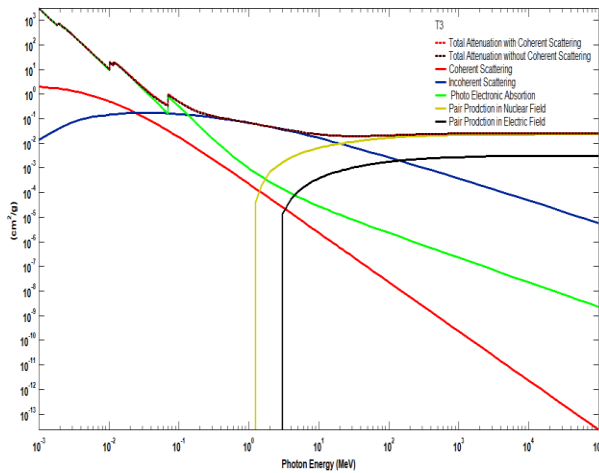


**Figure (4.11):-** Mass attenuation coefficient  $\mu_m(cm^2/g)$  as a function of the energy of the incident photon for sample( E1: PVA 0.75 + CH 0.225 + W 0.025) for the total and partial interactions.

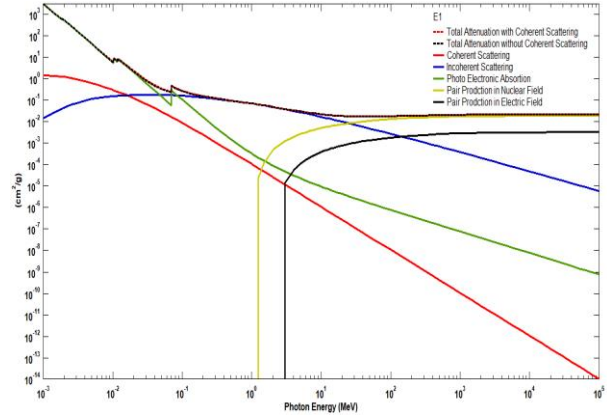


**Figure (4-12):** Mass attenuation coefficient  $\mu_m(cm^2/g)$  as a function of the incident photon energy for sample E2: PVA 0.75 + CH 0.20 + W 0.05)) for the total and partial reactions.

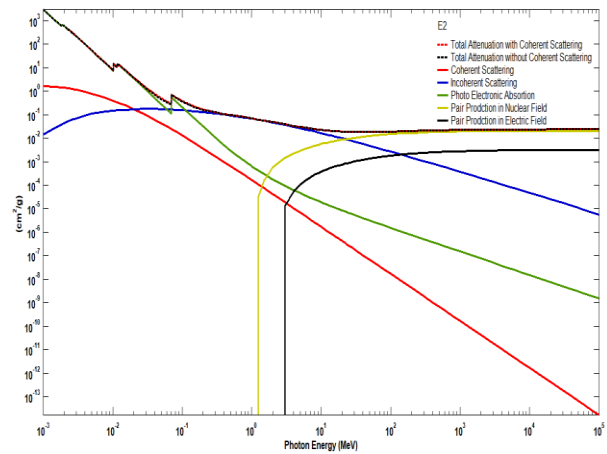


**Figure (4.13):** Mass attenuation coefficient  $\mu_m(cm^2\backslash g)$  as a function of the incident photon energy for sample E3: PVA 0.75 + CH 0>175 + W 0.075)) for the total and partial interactions.

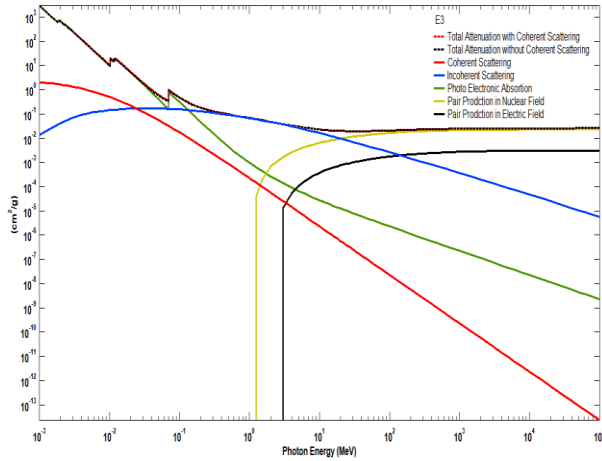


**Figure (4.14):** Mass attenuation coefficient  $\mu_m(cm^2\backslash g)$  as a function of the incident photon energy for sample C1: PVA 0.85 + CH 0.10 + Cement 0.05)) for the total and partial interactions.

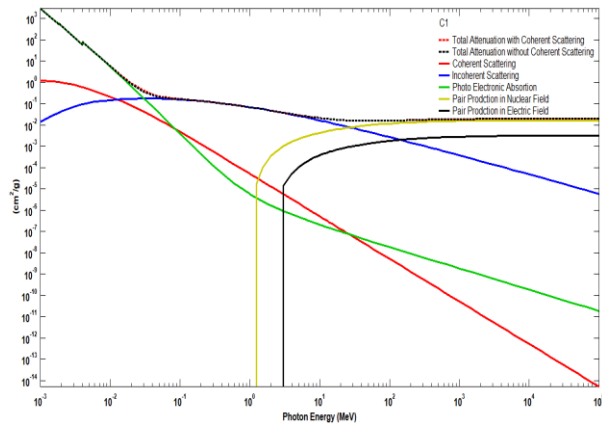


**Figure (4.15):** Mass attenuation coefficient  $\mu_m(cm^2\backslash g)$  as a function of the incident photon energy for sample (C2: PVA 0.80 + CH 0.10 + Cement 0.10) for the total and partial interactions.

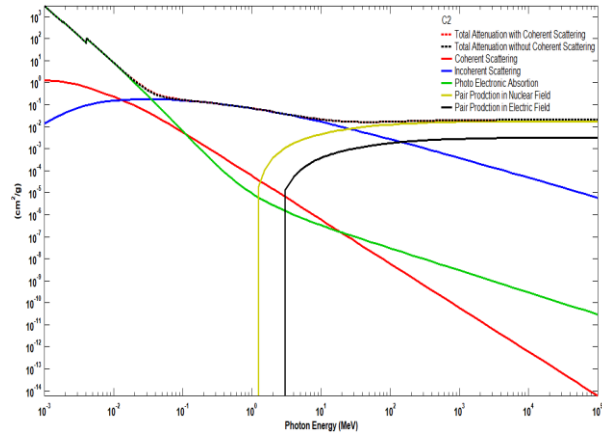


**Figure (4.16):** Mass attenuation coefficient  $\mu_m(cm^2\backslash g)$  as a function of the incident photon for the sample( C3: PVA 0.75 + CH 0.10 + Cement 0.15) for the total and partial reactions.

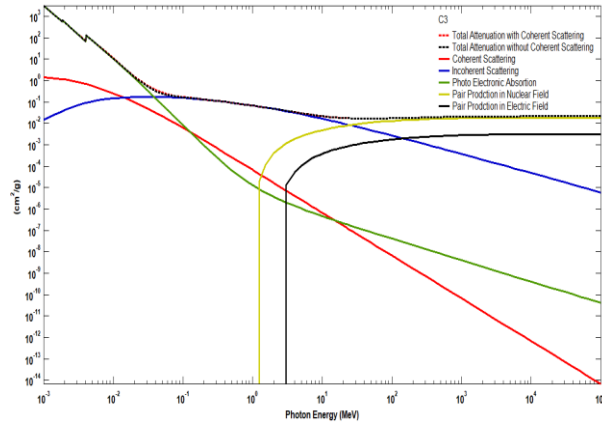


**Figure (4.17):** Mass attenuation coefficient  $\mu_m(cm^2/g)$  as a function of the incident photon energy for sample( M1: PVA 0.75 +St 0.20 +C 0.05) for the total and partial interactions.

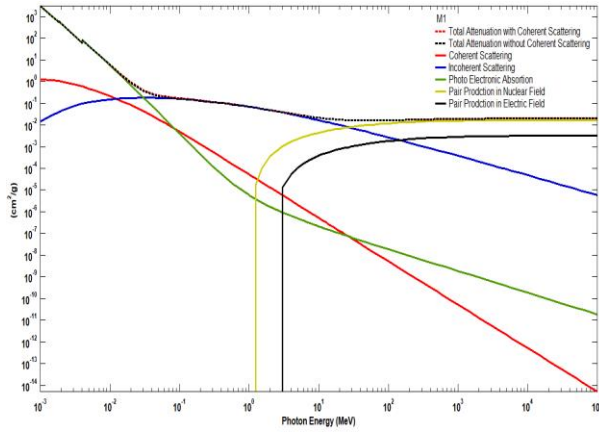


**Figure (4.18):** Mass attenuation coefficient  $\mu_m(cm^2/g)$  as a function of the energy of the incident photon of the sample(M2: PVA 0.70 +St 0.20 +C 0.10) for the total and partial reactions.

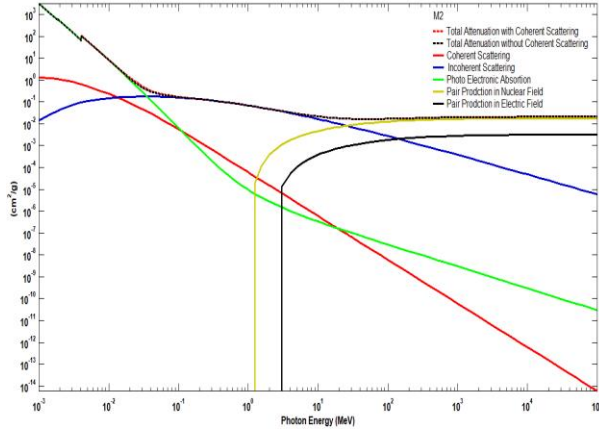


**Figure (4.19):** Mass attenuation coefficient  $\mu_m(cm^2/g)$  as a function of the incident photon energy for sample( M3: PVA 0.65 +St 0.20 +C 0.15) for the total and partial interactions.

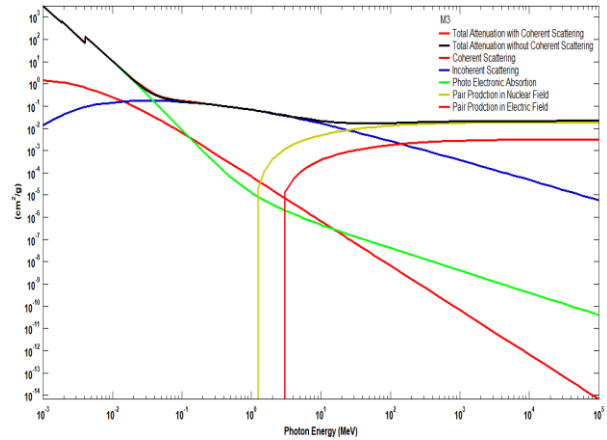


**Figure (4.20):** Mass attenuation coefficient  $\mu_m(cm^2/g)$  as a function of the incident photon energy of the sample (Control1:PVA 0.90 + CH 0.10) for the total and partial reactions.

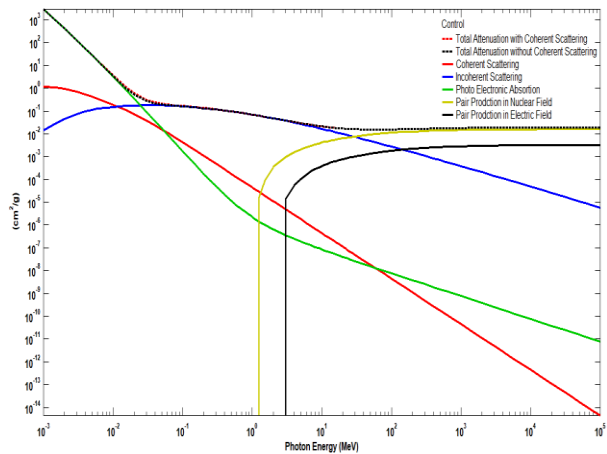


**Figure (4.21):- Mass attenuation coefficient  $\mu_m(cm^2\backslash g)$  as a function of the energy of the incident photon of the sample( Control2: PVA 0.90 + Starch 0.10) for the total and partial interactions.**

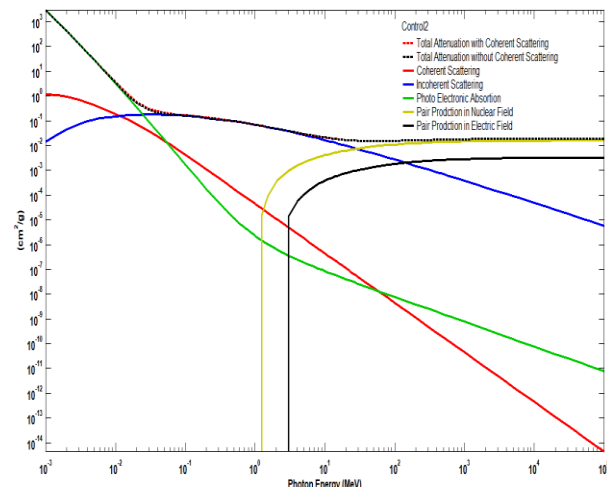


Table No. (2-4), demonstrating practical results for the total mass attenuation coefficient  $\mu_m$  and the linear attenuation coefficient for fourteen heterogeneous material samples for several popular gamma ray sources [Cs]  $^{137}(0.662\text{MeV})$  [Co]  $^{60}(1.1732\text{MeV}, 1.3325\text{MeV})$  and the average energy of these two values is (1.25 MeV), which is widely used in various purposes.

**Table (2-4): shows the total mass attenuation coefficient ( $\mu\backslash\rho$ ) and the linear attenuation coefficient  $\mu$  for a sample of different materials for some radiation sources.**

Sample ID	I (E=662 of Cs-137)	I (E=1173.5 of Co-60)	I (E=1332.25 of Co-60)	Thick ness x (cm)	density (g/cm <sup>3</sup> )	$\mu$ (662)(1/cm)	$\mu$ (1173)(1/cm)	$\mu$ (1332)(1/cm)	$\mu$ (cm <sup>2</sup> /g) (662)	$\mu$ (cm <sup>2</sup> /g) (1173)	$\mu$ (cm <sup>2</sup> /g) (1332)
control (PVA+c hitosan)	840993	15887	12409	0.042	0.855	0.203197607	0.10467714	0.130117468	0.23765802	0.122429398	0.152184173
E1	830553	15552	12332	0.038	1.55625	0.553312948	0.6765357	0.307616826	0.355542456	0.434721737	0.197665431
E2	833231	15484	12349	0.035	2.03	0.508763467	0.85972491	0.294624608	0.250622398	0.423509806	0.145135275
E3	832934	15406	12304	0.045	2.50375	0.403627304	0.78090134	0.310278593	0.161209108	0.311892699	0.123925549
C1	838475	15698	12214	0.04	1.2531	0.288321758	0.40910722	0.532602866	0.230086791	0.326476114	0.425028223
C2	830201	15321	12069	0.065	1.2962	0.329996859	0.62574105	0.511488735	0.254587918	0.482750384	0.394606338
C3	830673	15409	12345	0.08	1.3393	0.261017755	0.43682313	0.132947833	0.194891178	0.326157789	0.099266656
control	813848	15311	3447	0.065	1.405	0.63606184	0.63578585	19.79050249	0.452713054	0.452516618	14.0857669
T1	800957	15466	2727	0.12	1.80375	0.477586444	0.26044615	12.67237371	0.264774189	0.144391491	7.025571012
T2	801343	15646	2917	0.1	2.25	0.568285659	0.19682311	14.53331259	0.252571404	0.087476939	6.459250038
T3	805829	15755	3887	0.108	2.269625	0.474500693	0.11796138	10.79860461	0.209065679	0.051973952	4.757880534
M1	800882	15421	11714	0.116	1.3906	0.494862204	0.29454644	0.543984843	0.355862364	0.211812487	0.391187144

M2	809100	15154	12091	0.108	1.4332	0.436991826	0.47808408	0.290977 548	0.304906 381	0.3335780 65	0.2030264 78
M3	801299	15124	11521	0.12	1.4758	0.47402896	0.44678932	0.664295 77	0.321201 355	0.3027438 14	0.4501258 77

**Reference**

[1]" 'R. Biswas, H. Sahadath, A. S. Mollah, and M. F. Huq, "Calculation of gamma-ray attenuation parameters for locally developed shielding material: Polyboron," J. Radiat. Res. Appl. Sci., vol. 9, no. 1, pp. 26–34, 2016.'."

[2]" 'ICRU (1984). International Commission on Radiation Units and Measurements. ICRU Report 37, Stopping Powers for Electrons and Positrons.'."

[3]" 'Robley D Evans (1955), Chapter-25, The Atomic Nucleus, Tata McGraw- Hill Inc., New York.'."

[4]" 'Elmahroug, Y., Tellili, B., & Souga, C. (2013). Calculation of gamma and neutron shielding parameters for some materials polyethylene-based. International Journal of Physics and Research, 3, 33e40'."

[5]" K. D. Ianakiev, B. S. Alexandrov, P. B. Littlewood, and M. C. Browne, 'Temperature behavior of NaI(Tl) scintillation detectors,' Nucl. Instruments Methods Phys. Res. Sect. A Accel. Spectrometers, Detect. Assoc. Equip., vol. 607, no. 2, pp. 432–'."

[6]" I. Akkurt, K. Gunoglu, and S. S. Arda, "Detection efficiency of NaI(Tl) detector in 511-1332 keV energy range," Science and Technology of Nuclear Installations, vol. (2014).'."

[7]" K. S.Krane, "Intro. Nuclear Physics (libro rojo)," Foreign Aff., vol. 91, no. 5, pp. 1689–1699, (2012).'."

[8]" J. L. Duggan, "Experiment 3 Gamma-Ray Spectroscopy Using NaI(Tl)," AN34

laboratory manual, vol. 1, no. 3. pp. 1–20, (2010). ['."

[9] 'SICS. A. O. MUSTAPHA, "STUDY MATERIAL PHS451 NUCLEAR PHY"'."